

## **Augmentation of Early Intensity Forecasting in Tropical Cyclones**

J. Scott Tyo

College of Optical Sciences

University of Arizona

Tucson, AZ 85721

Phone: (520) 626-8183 FAX: (520) 621-4358 E-mail: [tyo@optics.arizona.edu](mailto:tyo@optics.arizona.edu)

Elizabeth A Ritchie

Department of Atmospheric Sciences

University of Arizona

Tucson, AZ 85721

Phone: (520) 626-8183 FAX: (520) 621-6833 E-mail: [ritchie@atmo.arizona.edu](mailto:ritchie@atmo.arizona.edu)

Award Number: N00014-10-1-0146

<http://www.optics.arizona.edu/asl>

### **LONG-TERM GOALS**

The long-term goals of our research team are twofold:

1. To develop a suite of objective intensity estimation tools that are based on remote sensing data and multiparameter spatiotemporal analysis tools.
2. To understand the physical mechanisms giving rise to the observable signatures that are used for forecasting.

### **OBJECTIVES**

Our principal objective is to develop an objective and automatic intensity estimator of Tropical Cyclones (TCs) based on satellite infrared (IR) imagery. The proposed methodology analyzes the TC's structure to estimate their intensity, which will be available every 30 minutes (or depending on image acquisition availability) for the Atlantic, Eastern North Pacific and Western North Pacific basins. We are investigating the underlying atmospheric dynamics by using mesoscale modeling and comparing the modeled storms to the measured signatures.

### **APPROACH**

The deviation-angle variance (DAV) technique was introduced in Pineros et al. (2008) as a procedure to objectively estimate the intensity of tropical cyclones. The level of axisymmetry of tropical cyclones is quantified by calculating the gradient of the brightness temperature field in infrared images. The deviation-angle of these gradient vectors with respect to a radial line projected from a center indicates their level of "alignment". Fig. 1a shows an example of this calculation for a single gradient vector in a brightness temperature field. In this case the center is located at the eye of the vortex. The calculation is done for every pixel within a chosen radius of the center point, and the variance of the distribution of angles quantifies the axisymmetry of the cyclone (Fig. 1b). The deviation-angle variance decreases as the majority of gradient vectors are pointing toward or away from the center. In contrast, the DAV increases when the orientation of the vectors is disorganized, which is characteristic of regular non-

| Report Documentation Page  |                                    |                                     |   | Form Approved<br>OMB No. 0704-0188          |                                    |
|--|------------------------------------|-------------------------------------|---|---|------------------------------------|
| Public reporting burden for the collection of information is estimated to average 1 hour per response, including the time for reviewing instructions, searching existing data sources, gathering and maintaining the data needed, and completing and reviewing the collection of information. Send comments regarding this burden estimate or any other aspect of this collection of information, including suggestions for reducing this burden, to Washington Headquarters Services, Directorate for Information Operations and Reports, 1215 Jefferson Davis Highway, Suite 1204, Arlington VA 22202-4302. Respondents should be aware that notwithstanding any other provision of law, no person shall be subject to a penalty for failing to comply with a collection of information if it does not display a currently valid OMB control number. |                                    |                                     |   |   |                                    |
| 1. REPORT DATE<br><b>2012</b>  |                                    | 2. REPORT TYPE<br><b>N/A</b>        |   | 3. DATES COVERED<br><b>-</b>                |                                    |
| 4. TITLE AND SUBTITLE<br><b>Augmentation of Early Intensity Forecasting in Tropical Cyclones</b>   |                                    |                                     |   | 5a. CONTRACT NUMBER                         |                                    |
|  |                                    |                                     |   | 5b. GRANT NUMBER                            |                                    |
|  |                                    |                                     |   | 5c. PROGRAM ELEMENT NUMBER                  |                                    |
| 6. AUTHOR(S)   |                                    |                                     |   | 5d. PROJECT NUMBER                          |                                    |
|  |                                    |                                     |   | 5e. TASK NUMBER                             |                                    |
|  |                                    |                                     |   | 5f. WORK UNIT NUMBER                        |                                    |
| 7. PERFORMING ORGANIZATION NAME(S) AND ADDRESS(ES)<br><b>College of Optical Sciences University of Arizona Tucson, AZ 85721</b>  |                                    |                                     |   | 8. PERFORMING ORGANIZATION<br>REPORT NUMBER |                                    |
| 9. SPONSORING/MONITORING AGENCY NAME(S) AND ADDRESS(ES)  |                                    |                                     |   | 10. SPONSOR/MONITOR'S ACRONYM(S)            |                                    |
|  |                                    |                                     |   | 11. SPONSOR/MONITOR'S REPORT<br>NUMBER(S)   |                                    |
| 12. DISTRIBUTION/AVAILABILITY STATEMENT<br><b>Approved for public release, distribution unlimited</b>  |                                    |                                     |   |   |                                    |
| 13. SUPPLEMENTARY NOTES<br><b>The original document contains color images.</b>   |                                    |                                     |   |   |                                    |
| 14. ABSTRACT   |                                    |                                     |   |   |                                    |
| 15. SUBJECT TERMS  |                                    |                                     |   |   |                                    |
| 16. SECURITY CLASSIFICATION OF:  |                                    |                                     | 17. LIMITATION OF<br>ABSTRACT<br><b>SAR</b> | 18. NUMBER<br>OF PAGES<br><b>17</b>         | 19a. NAME OF<br>RESPONSIBLE PERSON |
| a. REPORT<br><b>unclassified</b>   | b. ABSTRACT<br><b>unclassified</b> | c. THIS PAGE<br><b>unclassified</b> |   |   |                                    |

developing cloud clusters. The point of reference was chosen by calculating the variance of the distribution of the deviation angles for every point in the scene (Pineros et al. 2010). Fig. 1c shows an example of the map of variances. Selecting the minimum DAV in the maps produces a suboptimal value in dense overcast clouds, reason why in this study the center is determined by the best-track center estimates.

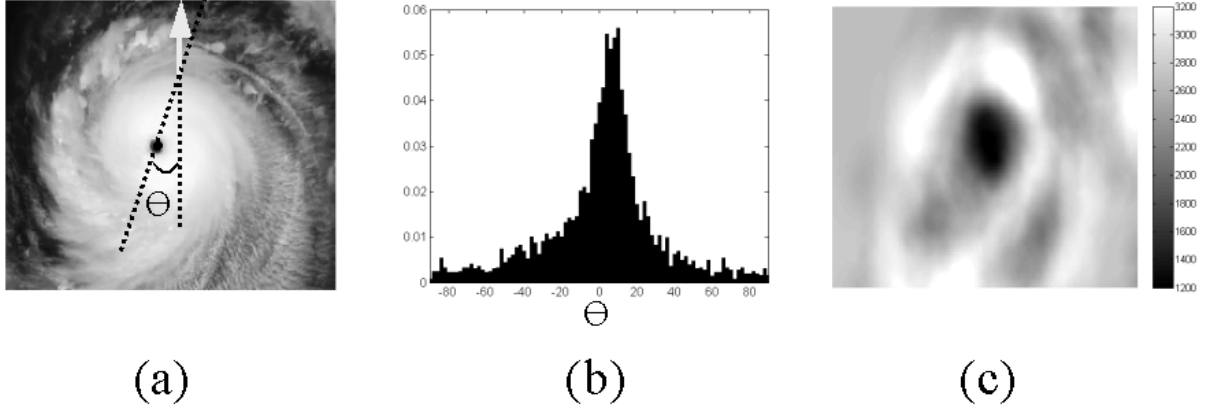


Figure 1. IR image of the Western North Pacific at 1230 UTC October 04, 2010. The image includes Typhoon Melor (72 m/s, 911 hPa): a) Deviation-angle calculation for a single gradient vector, the center is located at the eye of the tropical cyclone; b) Distribution of angles, the variance is 1216 deg<sup>2</sup>; c) Map of variances [deg<sup>2</sup>]

As described in Pineros et al. (2011), eight different radii varying from 150 km to 500 km in steps of 50 km were used to calculate the DAV signals, which are smoothed with a single-pole low pass filter (impulse response:  $e^{-kt}$ ) of  $0.01 \pi$  rad/sample cutoff frequency (filter time constant of 100 h). After processing all the samples, the data set is divided into two groups. The first subset is used as a training set to calculate the parametric curve; the second subset tests the wind speed estimator. Fig. 2 shows the two-dimensional histogram of the filtered DAV samples (radius of 250 km) versus the best-track intensity for 40 tropical cyclones during 2007 and 2008. A sigmoid (Eq. 1) is fitted to obtain the parametric curve that describes the relation between the two variables (Fig. 2, black curve). Note that the minimum intensity allowed is 25 kt (12.86 m/s) and the maximum is 165 kt (84.9 m/s).

$$f(\sigma^2) = \frac{140}{1 + \exp(\alpha(\sigma^2 + \beta))} + 25 \quad [kt], \quad (1)$$

The intensity estimation is performed by calculating new filtered DAV signals and applying the parametric curve obtained in the training phase. Beginning in year 2 of the effort we implemented a supervised center location method whereby best track centers (or other center locations provided by a user) could be input to localize the computation (Ritchie, *et al.*, 2012), and this method has been extended to all three basins as our default processing strategy.

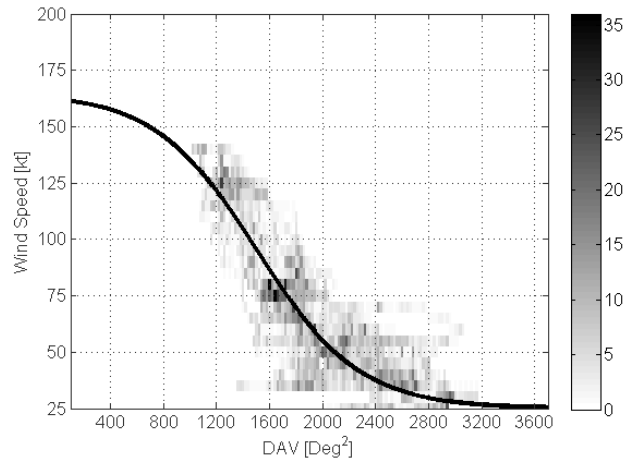


Figure 2. Two-dimensional histogram of the 250-km filtered DAV samples and best-track intensity estimates using 20-deg x 5-kt bins for 40 tropical cyclones of 2007 and 2008 in the Western North Pacific basin. The black line corresponds to the best-fit sigmoid curve for the median of the samples.

The development of a tropical cyclone intensity estimator for each ocean basin consists of the following tasks:

1. IR satellite imagery database construction
2. DAV signal calculation per TC
3. DAV-Intensity Parametric curve calculation
4. Testing the obtained parametric curve (estimator) with a different data set

The team at the University of Arizona is composed of the following members (*italicized members are no longer working on the project*):

- J. Scott Tyo, PI, (Optical Sciences – Professor)
- Elizabeth A. Ritchie, co-PI (Atmospheric Sciences - Professor)
- Klaus Dolling (Postdoc) Observational aspects of the program, TC structure and DAV
- Oscar Rodríguez-Herrera (Postdoc) Development of improvements to the DAV system including automatic processing for the WestPac and development of automatic tracking algorithms.
- Kim Wood (ATMO - Ph.D. Student/Postdoc): Construction of the image database, development of the intensity estimator and real-time application for the eastern North Pacific basin, development of automatic processing methodology for Atlantic and Eastern North Pacific.
- Wiley Black (Optics - Ph.D. Student): Website application design
- Kelly Ryan (ATMO – M.S. Student): Synthetic image generation from mesoscale model data and mesoscale modeling.
- *Miguel F Pineros (Postdoctoral associate, Optics, left UA in 2011): Construction of the image database, development of the intensity estimator and real-time application for the western North Pacific basin.*
- *Genevieve Valliere-Kelley (University of Arizona, M.S. Student, Graduated 2011): Incorporated best-track center fixes to improve intensity estimates; initial development in the eastern North Pacific basin.*
- *Brian LaCasse (Optics – Undergrad, Graduated 2011): Preprocessing of MTSAT data*

- *Arun Ganesan (ECE – Undergrad, Graduated 2011): Processing of GOES data*

The team at the Naval Research Laboratory –MRY is composed of:

- Mr. Jeffrey Hawkins (NRL – MRY)
- Mr. Richard Bankert (NRL -- MRY): Restore all available MTSAT data files from the NRL archive. Each restored file is then processed to netCDF format and placement on an ftp site for retrieval by UA and further processing.

The team members at JTWC – Honolulu are:

- Mr. Matthew Kucas (JTWC – Tech Development): assess genesis and intensity estimates for operational use in the western North Pacific. Assess website for operational utility
- Mr. James Darlow (JTWC – Tech Development):

The team members at NHC – Miami are:

- Mr. James Franklin(Branch Chief – Hurricane Specialist Unit): assess genesis and intensity estimates for operational use in the North Atlantic. Assess website for operational utility

Upcoming year work plan, tasks to complete:

1. Testing of the DAV method for genesis in the eastern North Pacific (UA)
2. Operational pre-testing of the DAV for genesis in the western North Pacific (UA, JTWC)
3. Completion of automatic system tracker and manual database interface for website application.
4. Detailed analysis of a subset of Atlantic cases where reconnaissance data are available in order to assess the ability of the DAV method to model structure.
5. Use of synthetic image data from model runs to assess high temporal frequency DAV results.
6. Extension of the DAV database to include Australian basins.

## **WORK COMPLETED**

Third year work completed includes:

- The data process flow for the western North Pacific was finalized, and the results for intensity and genesis were published.
- The intensity estimator was developed and tested in the eastern North Pacific Basin.
- Synthetic images were generated using WRF for model runs of real cases and DAV signals were extracted .
- The website interface was developed and published, and automatic processing methods were developed in order to publish DAV data in real time in the Atlantic and western North Pacific basins.
- An automatic disturbance tracking system was developed in the western North Pacific to aid in the genesis detection and forecasting routine.
- Preliminary results were obtained comparing spatial distribution of DAV signals to storm structure from reconnaissance data.

## **RESULTS**

### ***Western North Pacific Basin***

#### ***Cyclogenesis Detection***

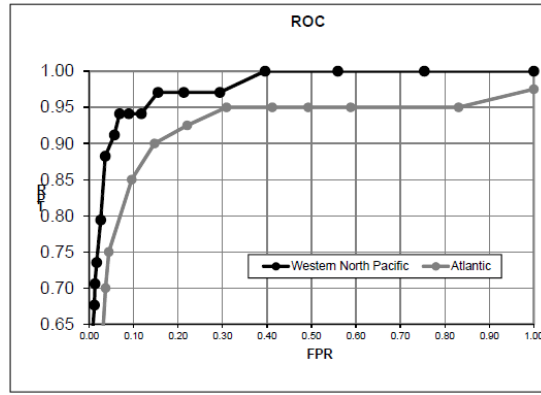


Figure 3. ROC curves for the WestPac and Atlantic for detection of tropical cyclogenesis

Cyclogenesis detection begins by computing a map-of-variances computed at every pixel (Piñeros, et al., 2010). All points within the image that fall below a user-defined threshold are highlighted as “detected” events. These systems are then followed through time; those that eventually designated TCs by the JTWC are termed “correct detections” and those that dissipate without forming are termed “false alarms.” In addition, DAV detections are also checked in the IR image for a minimum brightness temperature average within a fixed radius of 250km. This reduces the number of false alarms by removing those detections from dark regions (high temperature) in the IR image (threshold was calculated as one-third of the maximum pixel value to the entire scene average). The method as currently applied uses no additional information to eliminate false alarms, so the numbers presented here are upper bounds to the false alarm rates that could be expected when DAV-T is used by an expert observer. Changing the threshold value from 1250 – 2000 deg<sup>2</sup> produces a set of points that can be plotted on a Receiver Operating Characteristic (ROC) curve as shown in Fig. 3.

For each correct detection, the detection time from DAV-T is compared to the TD designation time from JTWC. Negative values mean that DAV-T flagged the storm before the operational center for that threshold. High threshold values represent low levels of axisymmetry, which might be found in non-developing cloud clusters. Use of high thresholds produces high number of false alarms but also early detection times. In contrast, low threshold values require well-organized cloud clusters typically found in already developed tropical cyclones. This reduces the number of false alarms but also delays the detection time.

### *TC Intensity Estimation*

As described in Pineros et al. (2011), the DAV values are obtained at a point by considering the deviation angles of the gradient vector within a pre-defined radius from that point. We expected that the DAV-T parameters would need to be adjusted from those chosen for the Atlantic, so eight different radii varying from 150km to 500km in steps of 50km were used. The DAV time series is smoothed with a single-pole low pass filter (impulse response:  $e^{-kt}$ ) of  $0.01 \pi$  rad/sample cutoff frequency (filter time constant of 100h). The filtering is done in order to reduce high frequency oscillations in the DAV time series for comparison with the interpolated best track intensity estimates.

After computing the DAV values at the centers from the best track database, the data set is divided into two groups. The first subset is used to calculate a parametric curve that relates the TC intensity with the DAV; the second subset tests the accuracy of the wind speed estimate produced by this parametric

curve. The model we use is a sigmoid with two free parameters that describes the relation between the axisymmetry with the JTWC best-track intensity estimates (Eq. 1).

The filtered DAV signals and the best-track intensity records are each interpolated to obtain 30-minutes time resolution. After being smoothed, the DAV signals and the best-track intensity records are mapped as explained in Pineros et al. (2011). Fig. 2 shows the two-dimensional histogram of the filtered DAV samples (radius of 250 km) and the best-track intensity for 40 tropical cyclones during 2007 and 2008. The parameters from Eq. 1 are fitted to minimize the mean square error from the data, producing  $0.0026 \text{ 1/deg}^2$  for  $\alpha$  and  $1504.5 \text{ deg}^2$  for  $\beta$ .

The intensity estimation is performed by calculating filtered DAV signals and applying the parametric curve obtained in the training phase. The minimum root mean square error (RMSE) for 12 tropical cyclones during 2009 is 15.7 kt (8.07 m/s). The RMSE is higher for intensities above 64kt (32.924 m/s); in particular the error is 19.2 kt (9.87 m/s) for intensities greater than 113kt (58.13 m/s). In contrast, for tropical storm intensities the RMSE is 13.75 kt (7.07 m/s). The RMSE for 80% of the samples is below 10.9 kt (5.6 m/s) and 13 kt (6.7 m/s) for 90% of them.

The large variety of tropical cyclone size and structure that exists in the predominantly monsoon trough environment in the western North Pacific presents a challenge for a scheme that measures the structure of the clouds. One solution is to find a way to automatically take into account the size of the storm either as an average over its life or at any instant in time. However, this is extremely challenging as there are no reliable, continuous measurements of the storm size currently available and our attempts to characterize size using the infrared brightness temperatures have met with little success thus far.

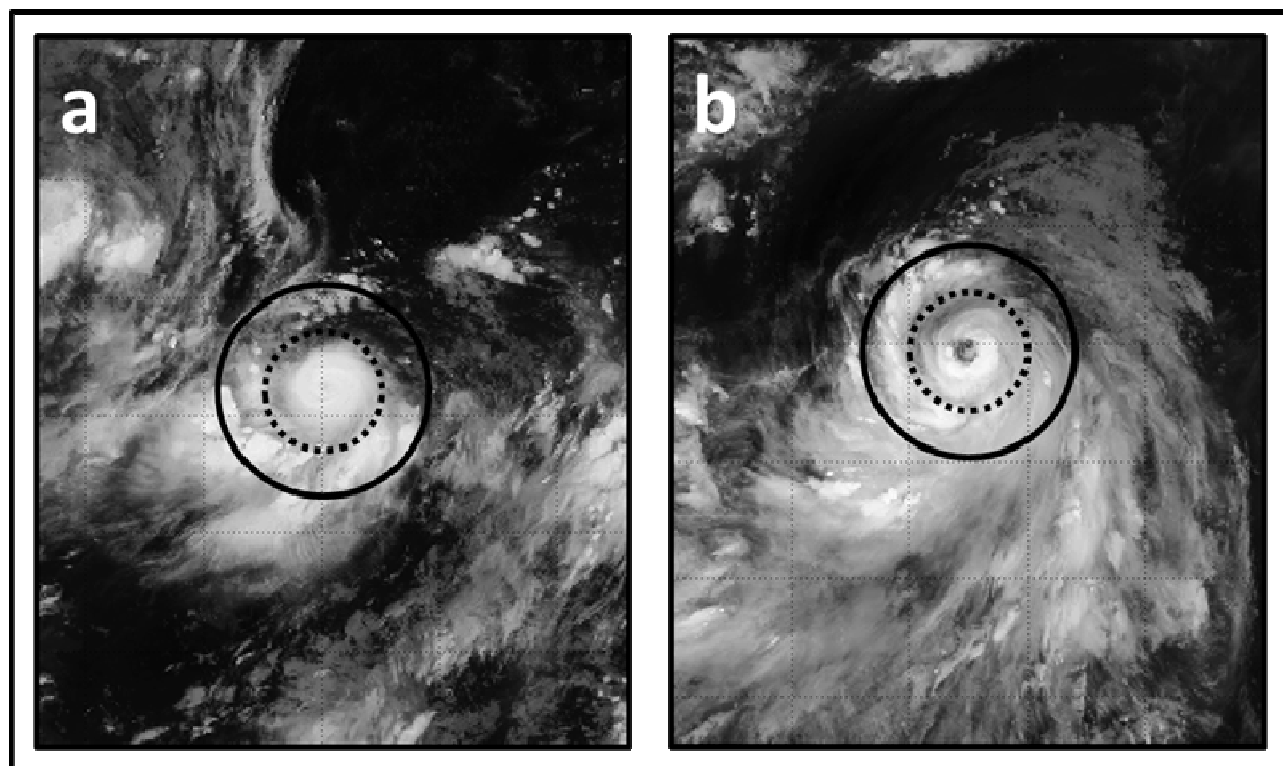


Figure 4. Infrared images of: a) Supertyphoon Sepat at 1630 UTC 14 August 2007. The current maximum sustained wind is 110 kt, and the central pressure is 941 hPa; and b) Typhoon Man-Yi at 1130 UTC 11 July 2007. Current intensity is 100 kt and the central pressure is 948 hPa. The circles indicate the 250-km (dashed) and 450-km (solid) radius respectively.

Figure 4 shows two examples of storms from 2007 (best overall performance radius of 300 km) that were best characterized by the DAV calculated over very different radii. Supertyphoon Sepat (Fig. 4a), was a small- to medium tropical cyclone characterized by a circular core of cold brightness temperatures, separated from, but embedded in monsoonal southwesterlies, and was best represented by a radius of 250 km. Using this small radius to train-test the DAV resulted in an RMS intensity error over the storm's lifetime of 13.3 kt compared with 18 kt using the "overall best" 300-km radius of calculation. Typhoon Man-Yi (Fig. 4b), was a medium- to large tropical cyclone characterized by spiral bands extending more than 500 km from the center of the storm. The best performance from the DAV was achieved using a radius of calculation of 400 km, which produced a lifetime RMS intensity error of 14.9 kt compared with 16 kt using a 300-km radius of calculation. Note that for Supertyphoon Sepat, a large radius of 400 km yielded an RMS intensity error of 32.3 kt while for Typhoon Man-Yi, a small radius of 250 km yielded an RMS intensity error of 17.2 kt. It appears that the size of the particular storm may have a bearing on the best radius over which to perform the DAV analysis. It is even plausible that as storms change size during their lifetime, a suitably varying radius of calculation may produce the most accurate DAV intensity estimates. This is an ongoing subject of research. Sifting through the entire dataset revealed that the western North Pacific tropical cyclones tended to fall into one of three categories: 1) those that were small and surrounded by peripheral monsoon cloudiness, and only did well with a radius of DAV calculation of 200-250 km; 2) those that were large, and only did well with a radius of DAV calculation of 400-500 km; and 3) those systems that showed no preference for a small or large radius of DAV calculation. In order to accommodate the first two classes of tropical cyclones, a set of DAV training data was specified using a combination of two radii calculation: a small radius and a large radius. A rectangular grid surrounding the entire set of training data was defined as an array of nodes to describe a two-dimensional fitted surface. The fitting



method works by expressing the value of the surface at points within the rectangular grid as a regularized linear regression problem, where the regularization is used to assure the existence of the solution when the number of grid points (i.e. the number of nodes) is larger than the number of sampling points. To build the original problem matrix, the surface value at the sampling points within the grid is expressed as a linear combination of the values that the fitted surface would have at the nodes surrounding the points. The linear combination is then written as a matrix. The regularization matrix is obtained by forcing the first partial derivatives of the surface in neighboring regions to be equal at the nodes. The two matrices are then coupled and the resulting system of linear equations is solved to find the surface value at the nodes (D’Errico 2006). The resulting 2-D parametric surface is shown in Figure 5 for a training set comprising all years and calculated using the DAV radii of calculation 250 and 500 km

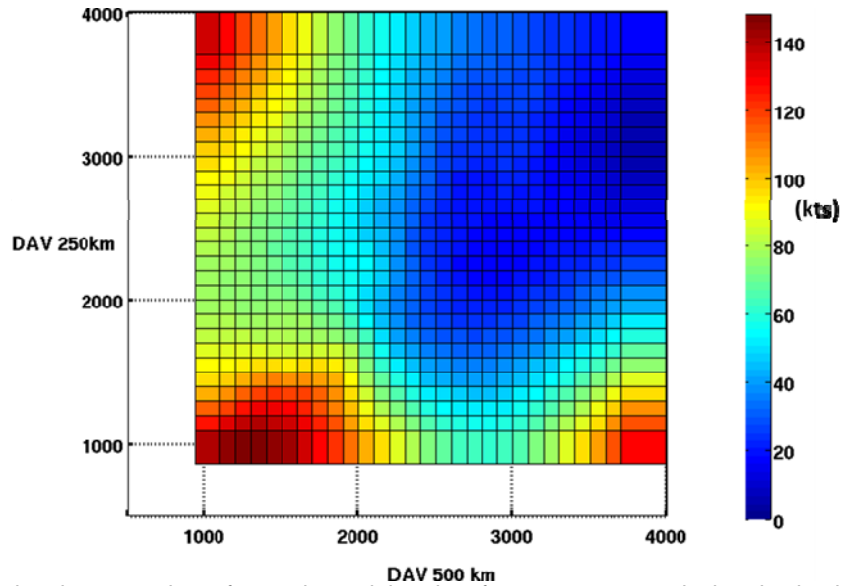


Figure 9: Two-dimensional parametric surface using training data from 2007-2011 calculated using both a 250-km radius of calculation and a 500-km radius of calculation. In order to estimate intensity, the DAV for an individual sample is calculated at both radii and then the intensity is extracted from the surface.

For testing purposes, all possible combinations of radii were tested to find the best performance. Table 1 shows the best performing radii when training and testing on all 89 storms as well as when performing independent testing on each year. Overall, the RMS intensity error improves from 14.3 kt with a training radius of 300 km, to 13.0 kt with a combination of 250- and 500-km training radius and a combination could be found that improved every individual year’s performance except for 2011. However, no single combination proved to be best for all years. RMS intensity errors for the two previous example tropical cyclones using radii of 250- and 500-km yields 12.7 kt and 21.2 kt for Typhoon Man-Yi (14.9 kt) and Supertyphoon Sepat (13.3 kt), respectively. Clearly for Sepat, the use of a 2-D surface was an impressive failure. However, for Man-Yi, the improvement over the “best training radius” RMS of 16 kt represents a respectable improvement, and there is an overall improvement for 2007 from 13.7 kt to 12.6 kt despite the degradation in Sepat’s performance.

### ***Eastern North Pacific Basin***

Like the North Atlantic studies, longwave (10.7  $\mu\text{m}$ ) IR images with a 4-km nadir resolution at 30 minute intervals were used in the eastern North Pacific basin intensity study. Again, these images were rectified to a Mercator projection and resampled to have a final resolution of 10 km per pixel. However, due to the limited coverage of the GOES-W satellite for the full eastern North Pacific basin,

GOES-W images were stitched together with GOES-E images post-resampling to cover the region 2.1° S to 39.3° N and 170.5° to 79.0° W. Note that GOES-W data are sampled at 00 and 30 minutes on the hour, while GOES-E data are sampled at 15 and 45 minutes on the hour, so there is a 15-minute difference between the two sides of each stitched image. The eastern North Pacific intensity study focuses on the 7-y period 2005-2011, providing a data set of 90 tropical cyclones. 6-h tropical cyclone best track data were again obtained from the NHC.

Eight radii, every 50 km from 150 km to 500 km, were used to calculate DAV intensity estimates for the eastern North Pacific intensity study. All samples at or above 15 kt were included. RMS intensity errors ranged from 9.3 kt to 15.5 kt for the individual years. Six of the seven years had a best training radius of 200 or 250 km. The seventh year, 2010, had a best training radius of 300 km, but this year also had the fewest TCs in the testing set (7) as it was the least active eastern North Pacific hurricane season on record (Cangialosi and Stewart 2011). The RMS intensity error computed for the seven-year period was 13.5 kt. 2007 produced the lowest error of 9.3 kt, and 2010 produced the highest error of 15.5 kt. Figure 6 shows the comparison between the DAV estimate and best track for the 2005 eastern North Pacific season using the other years as training data.

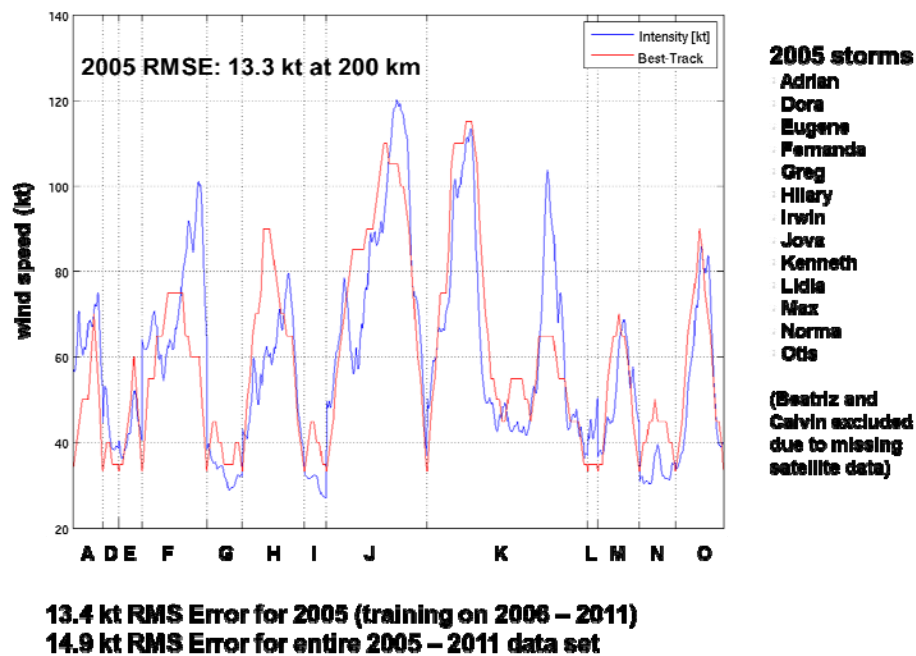


Figure 6. Comparison between the DAV estimate and the best track intensity for storms in the 2005 eastern North Pacific season.

### *Computation of DAV signal in model analysis*

In this project 11 cases of tropical cyclones from the 2005 North Atlantic hurricane season of varying intensities were simulated with the WRF-ARW model in order to produce hourly, fully consistent physical output with which to examine the DAV-intensity relationship. Initial results were calculated using out-going longwave radiation from the model output rather than brightness temperatures. The sigmoid fit to the data is shown in Figure 7.

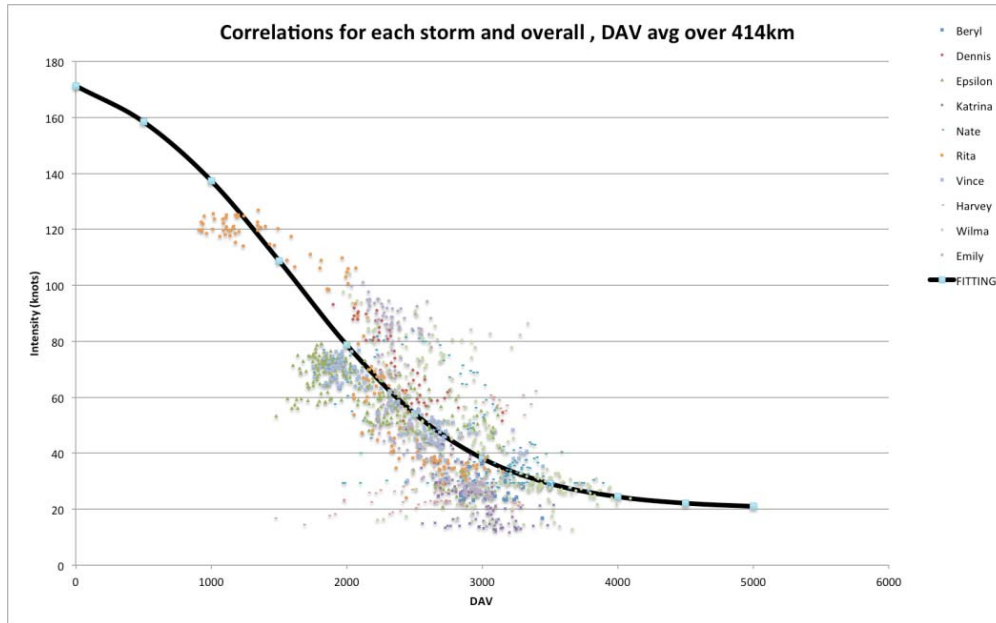


Figure 7: Scatter plot of intensity vs. DAV values for the azimuthal average out to a radius of 414 kilometers. The solid line is the sigmoid fit curve similar to that of Pineros et al. (2008).

Using the curve as an estimating tool, the estimated intensity of the simulated storms is plotted against the actual predicted values from the WRF model in Fig. 8. Although the RMS error appears rather high, these data include values at very early stages of cloud cluster evolution and may not be representative of true circulation values. We are currently re-analyzing the model output to remove obvious cases where these problems exist.

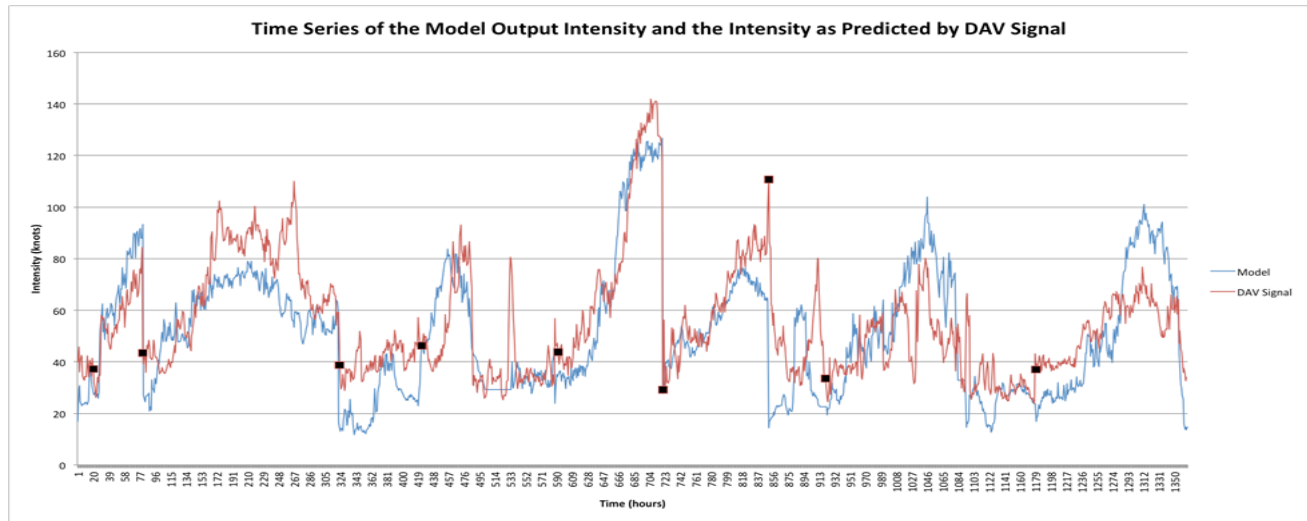


Figure 8: Time series of the maximum 10-m wind speed intensities as given by the WRF model output and as predicted by the DAV sigmoid curve. Black dots indicate a change in storm and are ordered alphabetically Overall RMS error is 18 kt.

### ***Development of the Real-Time DAV Web Interface***

The DAV method has been incorporated into a website interface which provides an opportunity for operational center forecasters and other users to evaluate and experiment with the method. The website contains an infrastructure which was designed to permit ease-of-use and extensibility, being a research environment where unanticipated changes were likely and future methods and investigations might also be presented. The website is available at <http://667-motherland.optics.arizona.edu>

The publicly accessible website contains archival data showing the DAV method calculated against storms from various years in the Atlantic and Western North Pacific basins. The “archival mode” presents best track markers against the geographic reference map with IR providing cloud imagery at a given time. DAV and genesis predictions can be overlaid on the map.

The website also incorporates a real-time mode which is accessible via password. The real-time mode incorporates satellite data received in near real-time for both the Atlantic and Western North Pacific. Genesis predictions are shown automatically, and DAV can be overlaid on the real-time maps. Intensity calculations with DAV are partially incorporated into the website, but have not gone live yet owing to a need for temporal filtering. Temporal filtering requires identifying a center location for each storm in order to assemble a time graph of the DAV signal. Two approaches are being developed in order to facilitate intensity estimation:

1. The new automatic tracking routine provides an automated, objective mechanism for identifying storm tracks in real-time.
2. Operational centers will provide invest lists in various file formats which can provide an analysis for an individual user.

We are working on integrating both methods into the website as we move forward. Investigators at Joint Typhoon Weather Center (JTWC) are presently evaluating the real-time DAV method and the web interface as forecast tools. We are using their feedback to improve and incorporate additional needed features into the web interface.

Additional future development includes incorporating the Eastern Pacific basin into the website. The web interface provides a useful research front-end where we can present the DAV methods and information from our research to operational centers as they become available before requiring a committed effort to modify their internal structures or systems. The web interface provides an infrastructure bridge between our research techniques and operational users with new developments in a low-risk environment.

### ***Automatic Disturbance Tracker for use in Genesis Prediction***

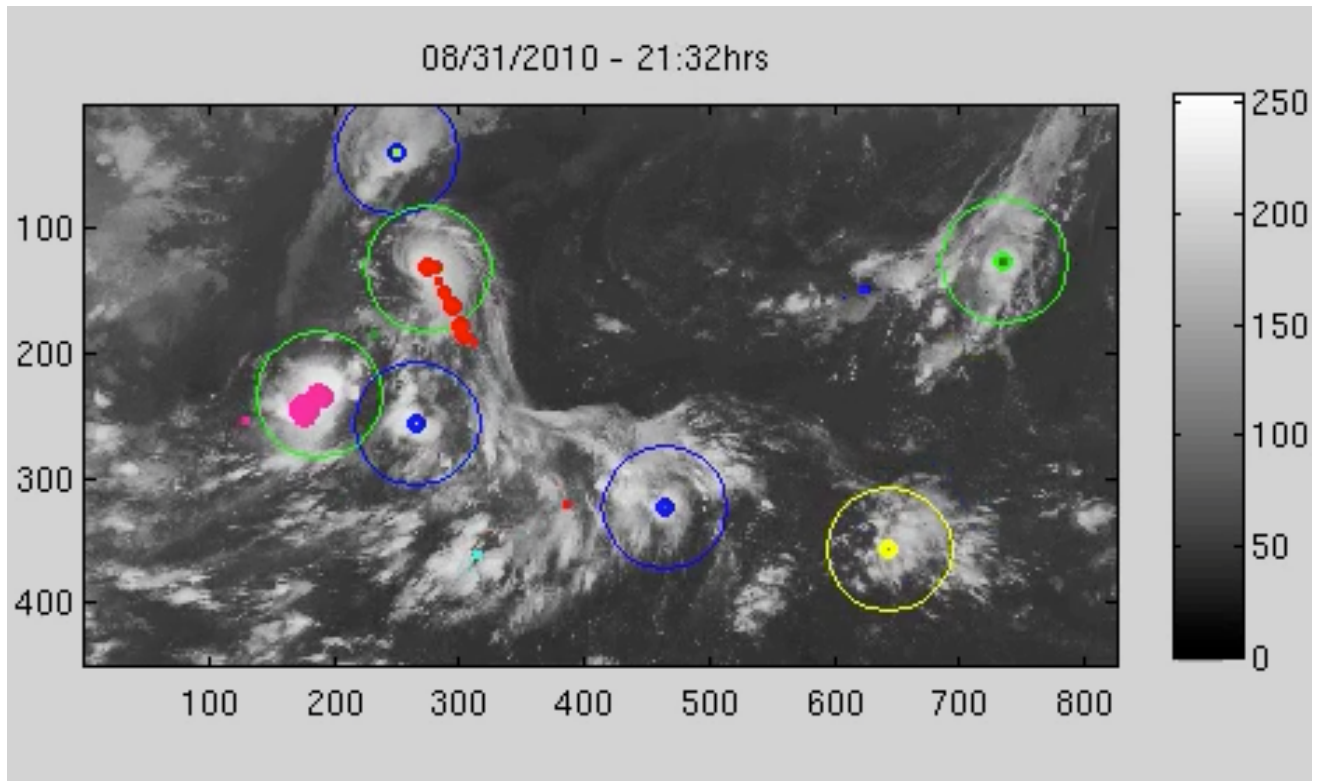
One of the main features of the DAV method is that the symmetry analysis of the cloud clusters is done in a subjective way. That is, the software implementation of the method calculates the DAV and returns a DAV value to the operator. Then, the operator must decide if a given detection belongs to a new potential storm developing in the basin of interest or is part of a previously identified storm that the operator is tracking. This part of the DAV analysis is done manually and thus, is sensitive to the expertise and ability of the operator, which may result in human errors that affect the final result of the DAV analysis. This is especially pronounced for “non-developing cases” that do not attain tropical depression status.

To reduce the dependance of the method on operator, we have developed an automatic tracking system that uses information from two different sources: the brightness temperature IR satellite image and its corresponding DAV map. First, the tracking system looks for regions on the DAV map with a variance below a given threshold  $TH_{max}$ . These regions correspond to highly symmetric regions in the IR image. Next it finds the pixels within those regions where the DAV is minimum. The location of those pixels is checked in the corresponding IR image to verify that a discernible cloud is present. It is necessary to check this since the DAV map contains only information about the symmetries within the IR image, ignoring the presence or absence of clouds in the basin. To define a discernible cloud, the

automatic tracking system computes the average brightness temperature in a circular region around the point of minimum DAV detected, and compares it with a minimum average brightness temperature threshold  $THB_{min}$ . Regions with a minimum DAV value below  $TH_{max}$  and an average brightness temperature above  $THB_{min}$  are labeled as true detections and included in a list that contains the minimum DAV value detected, the latitude and longitude of the point with that DAV value in the region of interest, the time and date of the detection, and a storm number that is used to label the different storms that might occur in the period of time under analysis. If any of the two thresholds is not reached, the point of minimum DAV is branded as a false detection and the automatic tracking system checks the true detections table for a previous true detection that might have been occurred in a circular vicinity of the new detection, with radius  $R_{track}$  within a time period  $T_{track}$ . If no previous true detection satisfying both conditions is found, the false detection is dismissed. Otherwise, the automatic tracking system includes the new detection's DAV value, latitude, longitude, date, time, and the storm number of the associated true detection in the true detections table in order to keep track of the cloud cluster in the event that no actual true detection is identified within a time period  $T_{track}$ . This is an important step because, due to the complex dynamics of cloud clusters, a storm being tracked might lose symmetry at some points in its evolution and then reorganize to continue developing. If either no true detection associated to a previous true detection is found within a period of time  $T_{track}$  or the average brightness temperature falls below  $THB_{min}$ , the storm is considered as finished and any new positive detection in the vicinity will be branded as a new storm and tracked in the same way as described above. The same process is repeated for all regions of minimum DAV found in the IR image. Then, the next image is loaded and analyzed in the same way. This process is repeated for all the imagery available in the period of time being analyzed.

Figure 9 is a snapshot of the automatic tracking system with a number of storms being tracked. The different colors represent the different storms that have been identified and are being tracked. The size of the dots is a function of the DAV value for each detection. Large dots correspond to low DAV values (high intensity) and small dots to high DAV values (low intensity). The path traced by a given storm as it travels across the basin, with a display persistence time of  $T_{track}$ , is represented by the set of dots with the same color. The circles in the image are centered in the point of minimum variance identified in the corresponding regions and are color coded to distinguish between true detections corresponding to new storms detected (blue), true detections corresponding to previously detected storms (green), and false detections associated to previously detected storms (yellow).

As part of the validation of the automatic storm tracking system we are running a test in which the performance of the system will be compared with a manual tracking done by two experts. This test will allow us to identify any inconsistency in the automatic tracking system and fine-tune the set of thresholds used in the tracking.



Snapshot of the automatic tracking system with several identified storms being tracked in the western North Pacific basin for the date and time indicated on the top of the image. The brightness temperature is given in an 8-bit digitized format (0--255). The latitude, vertical axis, and longitude, horizontal axis, are given in image pixels.

#### ***Use of DAV to extract storm structure***

The DAV method may have broader applications than tracking and intensity forecasts. As the radii used to calculate DAV increase, cloud areal average brightness temperatures tend to decrease, and there is a steady increase in the variance of the DAV. The spatial distribution of DAV measured at different radii changes depending on a storm's intensity and strength. Recent results in the western North Pacific have indicated that different radii of calculation yield better or worse results for different classes of storms (Ritchie, et al, 2013). In this study, we examine the spatial distribution of DAV and compare it to storm structure as determined in cases with significant aerial reconnaissance.

The “extended best-track file” (EBT) (Demuth et al. 2006) is an extension of the best-track data provided by the National Hurricane Center (NHC) (Neumann et al. 1999). The EBT consists of information on storm strength (intensity and size) as well as other variables. These variables include: the radius of maximum wind, radii of the 34, 50, and 64 kt wind to the northeast, southeast, southwest, and northwest of the TC. To attain the most accurate information from the EBT, only TCs that are continually monitored by aircraft reconnaissance are used in this study. EBT values must have reconnaissance data recorded within 3 hrs of the EBT time. We identified TCs in the EBT archive with semi-continuous reconnaissance for a period of at least 72 hrs. Six TCs were chosen because of the long period of continuous reconnaissance data. These include: Ivan (2004), Katrina (2005), Rita (2005), Ophelia (2005), Gustav (2008), and Ike (2008).

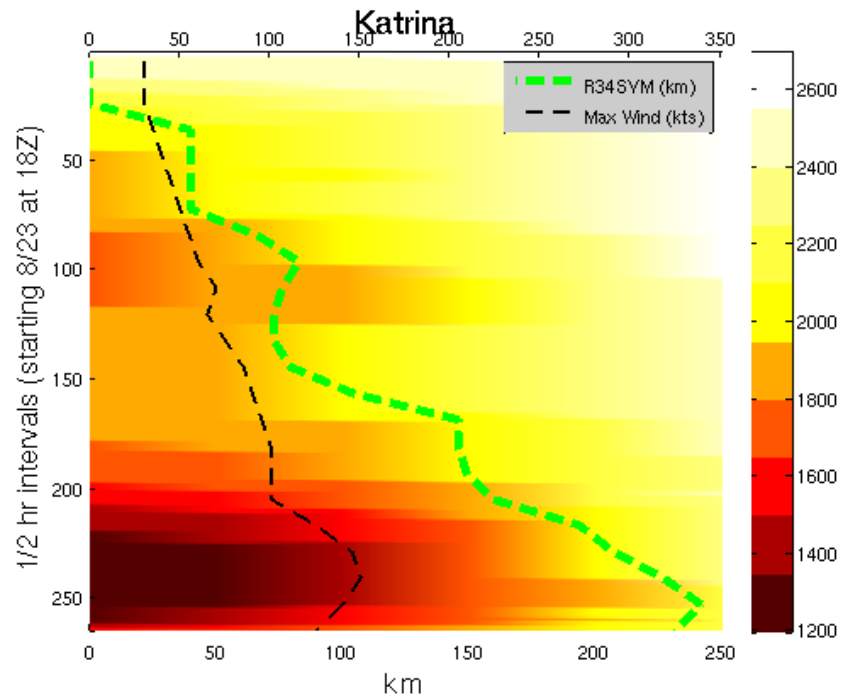


Figure 1 Plot of the deviation angle variance (DAV) structure of Katrina with time. Y-axis is the time at 1/2 hr intervals starting on 8/23/05 at 18 UTC. X-axis (bottom) is the radial distance from the TC center in which the DAV was calculated. DAV is calculated in 50 km radial bins from the TC center to the 250-300 km bin. Color bar displays the amount of variance for each radial bin DAV calculation. X-axis (top) displays the distance (km) from the TC center of the 34 kt symmetric winds around Katrina and the maximum sustained winds (kts) of Katrina from the extended best-track file.

We have calculated the EBT symmetric component of the wind at different radii. Also computed are the integrated symmetric DAV component for radial bins at increments of 10, 20 and 50 km. These values along with the radii of the 34, 50 and 64 kt winds are compared. An example is displayed in Figure 1 where the DAV signal is averaged in 50-km bins and compared with the radii of 34 and 50 knot winds for Katrina (2005). These calculations have been done for 4 of the 6 storms mentioned above. Numerous metrics will be explored to investigate if there is a statistically robust relationship between the variables in the EBT and the spatial distribution of DAV with a goal of constructing an objective technique to observe and record TC size and strength. Further study will investigate asymmetries in the EBT wind radii in concert with asymmetric components of the DAV technique to investigate if the asymmetries in a TCs wind field may be acquired from satellite data.

## IMPACT/APPLICATIONS

To estimate and predict the TC's intensity, forecast centers make use of in-situ measurements that are expensive and not always available. On the other hand, satellite-based imagery provides a key, reliable source of measurements over the data-sparse tropical oceans (e.g., Ritchie et al. 2003). Several procedures have been developed to estimate the TC's intensity from satellite imagery, among the most known ones are the Dvorak technique (Dvorak 1975), and the Advanced Dvorak Technique (ADT) developed by Olander and Velden (2007). Although the first technique is widely used, it is also subjective and produces quite different estimates depending on the operator. The second technique is



still being developed and has sensitive technical steps that can affect its performance (e.g. the TC pattern selection), but shows a lot of promise.

The technique developed in this research is simple, easy to implement, uses only infrared imagery, has a good performance, does not use pattern classification, and is a completely independent estimate of intensity. For this reason, this technique can enhance the actual TC intensity estimations generated by forecast centers around the world.

## **TRANSITIONS**

### **National Security**

We are working with our JTWC partners to test the DAV method for genesis assessment in the western North Pacific basin in the 2012 season.

### **Quality of Life**

Besides the papers published in scientific journals, a website application has been developed at the University of Arizona, which will be executed by and tested by the National Hurricane Center (NHC) and Joint Typhoon Warning Center (JTWC).

### **Science Education and Communication**

The co-PI organized a special symposium at the 2011 AMS Annual Meeting in Seattle focused on communicating information on hurricane science and hurricane forecasting to the public.

The PIs as well as several of the students and researchers working on this project are developing a pilot Adopt-A-School program in Tucson that focuses on STEM education in Title 1 Elementary Schools.

## **RELATED PROJECTS**

There are no currently funded projects directly related to this effort.

## **REFERENCES**

D'Errico, J., 2006: Understanding Gridfit, MATLAB Central.  
(<http://www.mathworks.com/matlabcentral/fileexchange/8998>)

Demuth, J., M. DeMaria, and J. A. Knaff, 2006: Improvement of advanced microwave sounder unit tropical cyclone intensity and size estimation algorithms. *J. Appl. Meteor.*, **45**, 1573-1581.

Dvorak, V. F., 1975: Tropical cyclone intensity analysis and forecasting from satellite imagery. *Mon. Wea. Rev.*, 103, no. 5, 420-430.

Neumann, C. J., B. R. Jarvinen, C. J. McAdie, and G. R. Hammer, 1999: *Tropical Cyclones of The North Atlantic Ocean, 1871-1998*. National Oceanic and Atmospheric Administration, 206 pp.

Olander, T. L. and C.S. Velden, 2007: The Advanced Dvorak Technique: Continued Development of an Objective Scheme to Estimate Tropical Cyclone Intensity Using Geostationary Infrared Satellite Imagery. *Wea. Forecasting*, 22, 287-298.



Piñeros, M. F., E. A. Ritchie, and J. S. Tyo, 2008: Objective Measures of Tropical Cyclone Structure and Intensity Change From Remotely Sensed Infrared Image Data. *IEEE Transaction on Geoscience and Remote Sensing*, 46, no. 11, 3574-3580.

Ritchie, E. A., J. Simpson, T. Liu, J. Halverson, C. Velden, K. Brueske, and H. Pierce, 2003: Chapter 12. Present day satellite technology for hurricane research: A closer look at formation and intensification. Hurricane! Coping with disaster, R. Simpson, ed. AGU Publications. 249-891.

Ritchie, E. A., G. Valliere-Kelley, M. F. Pineros, and J. S. Tyo, 2012: Tropical cyclone intensity estimation in the North Atlantic basin using an improved deviation angle variance technique. *Accepted for publication in Wea. Forecasting (In Press)*.

E. A. Ritchie, M. F. Piñeros, I. Darios-Hernandez, O. G. Rodríguez-Herrera, and J. S. Tyo, 2013 "Adaptation of Objective Intensity Estimator for Tropical Cyclones in the Western North Pacific," submitted to *Weather & Forecasting* September 2012 (*in review*)

Velden, C. S., B. Harper, F. Wells, J. L. Beven, II, R. Zehr, T. Olander, M. Mayfield, C. Guard, M. Lander, R. Edson, L. Avila, A. Burton, M. Turk, A. Kikuchi, A. Christian, P. Caroff, and P. McCrone, 2006a: The Dvorak tropical cyclone intensity estimation technique: A satellite-based method that has endured for over 30 years. *Bull. Amer. Meteorol. Soc.*, 87, 1195–1210.

Velden C. S., C. S., B. Harper, F. Wells, J. L. Beven, II, R. Zehr, T. Olander, M. Mayfield, C. Guard, M. Lander, R. Edson, L. Avila, A. Burton, M. Turk, A. Kikuchi, A. Christian, P. Caroff, and P. McCrone, 2006b: Supplement to: The Dvorak tropical cyclone intensity estimation technique: A satellite-based method that has endured for over 30 years. *Bull. Amer. Meteorol. Soc.*, 87, S6–S9.

## **PUBLICATIONS**

### *Journal Articles*

E. A. Ritchie, M. F. Piñeros, I. Darios-Hernandez, O. G. Rodríguez-Herrera, and J. S. Tyo, 2013 "Adaptation of Objective Intensity Estimator for Tropical Cyclones in the Western North Pacific," submitted to *Weather & Forecasting* September 2012

Ritchie, E. A., G. Valliere-Kelley, M. F. Pineros, and J. S. Tyo, 2012: Tropical cyclone intensity estimation in the North Atlantic basin using an improved deviation angle variance technique. To be published in *Wea. Forecasting*, Oct. 2012 (<http://dx.doi.org/10.1175/WAF-D-11-00156.1>).

Piñeros, M. F., E. A. Ritchie, and J. S. Tyo, 2011: Estimating Tropical Cyclone Intensity from Infrared Image Data. *Weather and Forecasting*, **26**:690 – 698

Pineros M. F., Ritchie E. A., Tyo J. S., 2010: Detecting Tropical Cyclone Formation from Satellite Infrared Imagery. 29th Conference on Hurricanes and Tropical Meteorology, Tucson, AZ, USA

Pineros, M. F., E. A. Ritchie, and J. S. Tyo, 2010: Detecting tropical cyclone genesis from remotely sensed infrared image data. *IEEE Geoscience and Remote Sensing letters*, **7**:826 – 830.

### *Conference Presentations*

Miguel F. Piñeros, Elizabeth A. Ritchie, J. Scott Tyo, Kim M. Wood, Genevieve Valliere-Kelley, Ivan Arias Hernández, Wiley Black, and Oscar Dominguez (2012), “Tropical Cyclone Intensity Estimation and Formation Detection using the Deviation Angle Variance Technique,” American Meteorological Society 30<sup>th</sup> Conference on Hurricanes and Tropical Meteorology, April 15-20, Ponte Vedra Beach, FL, USA.

Elizabeth A. Ritchie, Wiley Black, J. Scott Tyo, M. F. Pineros, Kimberly M. Wood, Oscar Rodriguez-Herrera, Matthew E. Kucas, and James W. E. Darlow, “A Web-based Interactive Interface for Researching and Forecasting Tropical Cyclone Genesis and Intensity using the Deviation Angle Variance Technique,” *2012 Interdepartmental Hurricane Conference*, Charleston, SC, March 2012

E. A. Ritchie, M. F. Piñeros, J. Scott Tyo, Kimberly M. Wood, Genevieve Valliere-Kelley, Wiley Black, Oscar Rodriguez-Herrera, and Ivan Arias Hernández, “Tropical Cyclone Intensity Estimation and Formation Detection using the Deviation Angle Variance Technique,” *2012 Interdepartmental Hurricane Conference*, Charleston, SC, March 2012